Boron carbides formed by coevaporation of B and C atoms: Vapor reactivity, B_xC_{1-x} composition, and bonding structure

I. Caretti,[1,*] R. Gago,[2] J. M. Albella,[1] and I. Jiménez[1]

[1]*Instituto de Ciencia de Materiales de Madrid (CSIC), C/ Sor Juana Inés de la Cruz 3, Cantoblanco, 28049 Madrid, Spain*
[2]*Centro de Micro-Análisis de Materiales (CMAM) and Departamento de Física Aplicada, Universidad Autónoma de Madrid, C/ Faraday 3, Cantoblanco, 28049 Madrid, Spain*

Boron carbides (B_xC_{1-x}) in thin film form have been synthesized in a high vacuum by coevaporation of B and C atoms from independent sources, allowing a study of the whole composition range from pure B films to pure C films. The relationship between the impinging B/C atomic fluxes and the film composition has been studied, providing information on the chemical reactivity between the B and C vapors. The composition was determined with x-ray emission energy dispersion spectroscopy and x-ray absorption near edge spectroscopy (XANES). Finally, the bonding structure of the films has been determined by XANES, showing a change from structures based on B_{12}-icosahedral units for the B-rich samples to hexagonal-like structures for the C-rich samples. The study shows that the structural transition takes place for $x \sim 0.5$.

I. INTRODUCTION

Borides and carbides hold an outstanding position in the framework of advanced ceramic materials due to their good mechanical, thermal, and chemical stabilities. A good combination of these three characteristics can be found in the group of covalent binary B_xC_{1-x} compounds, whose main representative material is stoichiometric boron carbide (B_4C).

B_4C is the third hardest existing material after diamond and cubic BN, and its collection of unique properties together with its relatively easy fabrication makes it suitable for many diverse applications such as bulletproof armor, rocket propulsion, neutron absorption, or abrasive powder. In the past decades, a large number of investigations have been devoted to the elucidation of the structure that is behind the properties of B_4C. Results using x-ray diffraction and absorption, neutron diffraction, nuclear magnetic resonance, and infrared and raman spectroscopies have been reported elsewhere.[1–7] Today, it is commonly accepted that its structure consists of 12-atom icosahedral units placed at the vertices of a rhombohedral unit cell and a linear chain of three atoms along the crystallographic *c* axis. This structure is known to be stable as long as the C incorporated is not higher than approximately 20%,[8] with variations in the composition of the icosahedra and the linear chain. Previous studies indicate that $B_{11}C$ icosahedra linked by CBC chains are typical of a B_4C composition.[9] For higher B percentages, the CBC chains are substituted by CBB chains and the mixed icosahedra are substituted by B_{12} units.[10] However, some details of the bonding structure still remain under debate. Namely, the number and position of C atoms in the icosahedrons, as well as in the three atom chain sequence linking them along the (111) rhombohedral axis, remain unclear. Therefore, recent studies have started to consider the simultaneous existence of several $B_{12-n}C_n$ "polytypes" with a random number *n* of C atoms in the polar and/or in the equatorial sites of the icosahedra to properly describe the structure and properties of boron carbide.[11]

Apart from B_4C, other boron carbides with higher C fractions or boron substituted carbon materials have also been investigated. In general, B_xC_{1-x} compounds with composition in the $0 < x < 0.25$ range draw attention due to the improvement in the oxidative resistance.[12] In this case, the basic underlying structure is expected to be hexagonal. For instance, a graphitelike BC_3 material was first synthesized in the 1980's (Ref. 13) and has been subjected to theoretical and experimental research.[14–16] Interestingly, very recently, the existence of a new superhard tetrahedral phase with the same composition has been predicted.[17]

Based on the electrical resistivity changes of amorphous B_xC_{1-x} (a-B_xC_{1-x}) compounds, it has been suggested that the B_4C-like structure is stable for C contents below 50%, consisting of a network of random icosahedra. When the C percentage is higher than 50%, a carbon-based network predominates.[18] Nevertheless, it is not clear if carbon is incorporated as part of the a-B_xC_{1-x} structure or if carbon segregation takes place.

In general, the investigation of B_xC_{1-x} compounds has been commonly carried out for a fixed composition or a short compositional range. In this work, we present a wider approach to understand the BC binary system by covering the whole compositional range from pure C to pure B. This was achieved for samples synthesized as thin films by using coevaporation in high vacuum with two independent sources for carbon and boron, which results in a good control of the growing parameters. In this way, we were able to relate the interaction of the carbon and boron atomic fluxes to the final composition of the coatings and its bonding structure.

II. EXPERIMENT

Boron carbide films were grown on Si(100) substrates by electron beam coevaporation of B and C pieces, with the substrate at room temperature and a working pressure of $< 10^{-6}$ mbar. Boron lumps of 99.5% purity and average volume of 0.2 cm^3 were fed and premelted in the crucible used for B evaporation. The carbon source was a 12 mm long

graphite rod with a diameter of 13 mm and a purity of 99% placed in the center of a carbon filled crucible. Evaporation from each source took place from a 9×9 mm^2 area irradiated with the e-beam. The substrates were cleaned *ex situ* in consecutive ultrasonic baths of acetone and ethanol before deposition. The two AP&T electron gun evaporators (models EVM-5 and EV1-8) were installed at 20 cm from each other and are able to reach electron beam intensities up to 500 mA for the acceleration voltage employed of 7 kV. The substrates were located at the central point between the evaporators, which is at a distance of 30 cm from the center of each crucible. The uniformity of the B and C atomic fluxes impinging the substrate was confirmed by measurement of the deposition rate at different emission angles. Atomic mixing of the B and C atoms by interdiffusion in the vapor phase and by surface diffusion at the substrate is expected, considering that the kinetic energy of the evaporated atoms is ~0.3 eV,[19] i.e., higher than the ~0.2 eV activation energy limit for surface diffusion.[20] The samples were grown at room temperature, avoiding intentional annealing that might break the low stability metastable phases into segregated graphite and B$_4$C phases.

The thickness of the films was estimated with a Dektak 3030 profilometer with a resolution of ~10 nm. The composition of the samples was determined by x-ray energy dispersive spectroscopy (XEDS) analysis with an EDAX® super-UTW microprobe (energy resolution at B, C, N, and O *K* edges of 50 eV) mounted on a Phillips XL30 ESEM scanning electron microscope. For quantification, we used the relative XEDS sensitivity factors (*k* factors) of B, C, and O as determined from the B$_4$C and B$_2$O$_3$ reference samples at several electron beam energies in the 1–10 keV range, as described in detail elsewhere.[21] Additional compositional information was obtained by x-ray absorption near edge spectroscopy (XANES) by using the height of the absorption jumps calibrated to the same reference samples. The composition values determined by both methods were in agreement within 5 at. %, which is considered as the experimental error bar. The oxygen contamination in the films was always below 2 at. %. The lateral compositional homogeneity of the films was confirmed by XEDS from several spots, and the in-depth homogeneity by XEDS at different electron beam energies.

The bonding structure of B$_x$C$_{1-x}$ coatings was studied by XANES at the beamline SA72 of LURE synchrotron in Orsay, France, and at the beamline PM4 of the BESSY-II facility in Berlin, Germany. All the spectra were recorded at room temperature in the total electron yield mode and at the magic angle with respect to the incident beam. The intensity was normalized to the signal detected from a gold covered grid. Reference samples of *h*-BN, *c*-BN, B$_4$C, graphite, and diamond were measured in the same conditions to calibrate the energy and sensitivity.

III. RESULTS AND DISCUSSION

A. Reactivity between B and C vapors in relationship with the film composition

The number of evaporated B and C atoms that reach the substrate per unit time and unit area is given by the expression
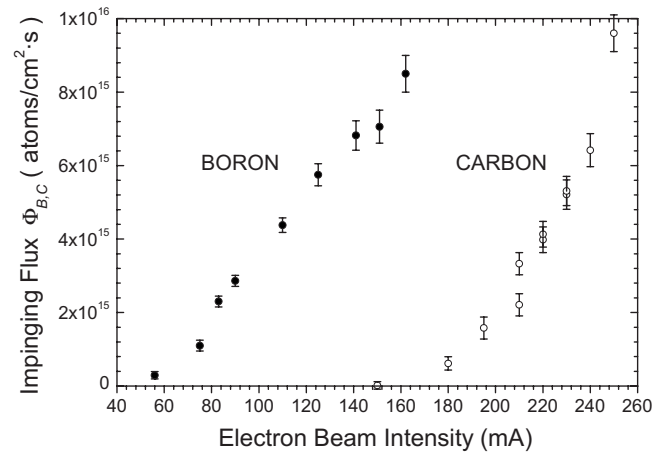
FIG. 1. Incident flux of evaporated boron and carbon atoms as a function of the electron beam intensity of the evaporators for a fixed electron acceleration voltage of 7 kV.

$$\Phi_{B,C} = (N_A \rho / A) V_d \quad (1)$$

where $\Phi_{B,C}$ represents the flux of B or C, N_A is Avogadro's number, ρ is the density of the element considered, A is the atomic mass, and V_d is the experimental deposition ratio, which is expressed as the thickness of a B or C layer grown per unit time.

The proportionality of the deposition rate to the atomic flux is based on two assumptions. First, the density of the B and C films is considered independent of their deposition rate. This is supported by the fact that the B and C films present an amorphous and dense growth without columnar or any other anisotropic atomic arrangement, hence allowing us to use the tabulated density of amorphous B and C for calculations herein.[22] Second, the sticking coefficient of the B and C atoms is considered as 1, i.e., all the impinging atoms contribute to the growing film. However, as we shall see along this paper, this assumption has to be revised for the case of carbon evaporation.

Under these considerations, the nominal impinging atomic fluxes were determined from the thicknesses of pure boron and carbon films grown at a fixed deposition time and different intensities of the electron beam evaporator, as indicated in Fig. 1. The error bars were calculated from the experimental uncertainty of the profilometer measurements. We observe that both fluxes of B and C increase with the intensity of the electron beam at a constant acceleration voltage of 7 kV. However, boron is more easily evaporated than carbon due to their differences in the evaporation temperature and heat diffusion. These calibration curves enable us to obtain good control over the final composition of the B$_x$C$_{1-x}$ compounds through a proper selection of the ratio of impinging B and C fluxes (Φ_B / Φ_C). The experiments were performed with a fixed nominal boron flux of $(4.5 \pm 0.5) \times 10^{15}$ at. cm^{-2} s^{-1} and varying the nominal carbon flux between $(15 \pm 0.6) \times 10^{15}$ and $(0.3 \pm 0.1) \times 10^{15}$ at. cm^{-2} s^{-1} to obtain flux ratios (Φ_B / Φ_C) between 0.3 and 15.

Figure 2 shows the composition of the binary B$_x$C$_{1-x}$ coatings measured by XEDS corresponding to several ratios
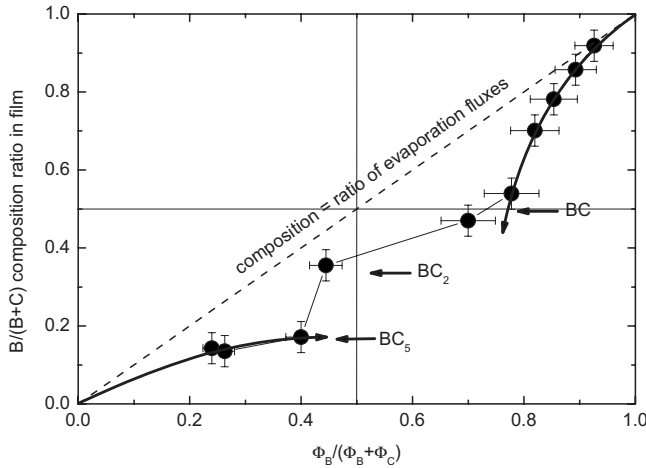
FIG. 2. Dependence of the film composition with the ratio of impinging atomic fluxes.

of evaporated fluxes. The compositional error indicated stems from the uncertainties in the XEDS intensities and sensitivity factors[21] and from the uncertainty in the deposition rate. The dashed line represents the 1:1 ratio of the relative film composition to the relative impinging fluxes. The experimental data show that such a situation is only found for pure carbon films (i.e., $\Phi_B/(\Phi_B+\Phi_C)=0$) and pure boron films (i.e., $\Phi_B/(\Phi_B+\Phi_C)=1$), with loss of boron in the films compared to the impinging fluxes in the intermediate situations. The maximum deviations between the flux ratios and the composition ratios are found when the films show (i) a BC_5 composition and (ii) a BC composition, the latter requiring using a boron flux Φ_B that is four times larger than Φ_C.

To fully understand this behavior, we need to take into account the reactivity of the species, that is, the physical and chemical mechanisms that occur at the deposition surface, and will determine the final stoichiometry of the binary BC compounds. The interaction between the boron and carbon atoms during the growth of boron carbides was studied by comparing the experimental deposition rate (V_d^{expt}) with the theoretical deposition rate (V_d^{theor}), the latter considered as the superposition of the individual atomic fluxes of each species. According to this, we define the normalized deposition rate (γ) as follows:

$$\gamma = V_d^{expt}/V_d^{theor}. \qquad (2)$$

Substitution of V_d from Eq. (1) into Eq. (2) for an arbitrary number of n evaporated species gives

$$\gamma = \sum K_i\alpha_i (i=1,\ldots,n), \qquad (3)$$

where $K_i=A_i\Phi_i^{inc}/\Sigma A_i\Phi_i^{inc}$ and α_i is the rate of adsorption of the evaporated atom i striking the substrate or *sticking coefficient*. The superscript "inc" refers to incident and A_i refers to the atomic mass of the i atom.

In accordance with this result, we can determine γ for each BC compound and the α coefficient of each atom participating in the deposit by just knowing the growth rate, the incident fluxes, the density of the material, and its composition. The density is the only parameter that has not been

experimentally measured. We have considered the density of the B_xC_{1-x} coatings (ρ_{BC}) as a linear combination of the boron (ρ_B) and carbon (ρ_C) densities: $\rho_{BC}=[\beta_{BC}/(\beta_{BC}+1)]\rho_B+[1/(\beta_{BC}+1)]\rho_C$, where β_{BC} represents the relative XEDS composition B/C. Since the densities of the reference materials graphite (2.25 g cm^{-3}), boron (2.45 g cm^{-3}), and B_4C (2.5 g cm^{-3}) are rather similar[22] and both parameters γ and α_i are proportional to ρ, the errors due to changes in the density of the B_xC_{1-x} coatings are minor.

The parameters γ and α_i ($i=B,C$) are represented in Figs. 3(a) and 3(b), respectively, as a function of the composition ratio B/(B+C) of the films. As it is expected, both γ and α_i ($i=B,C$) tend to 1 in the limits of pure B and pure C samples.

We observe that γ is greater than 1 when the carbon concentration in the films is high [B/(B+C)<0.4], indicating that the experimental deposition rate is higher than the one expected from the superposition of the incident atomic fluxes. In fact, according to the α_C values in the lower panel, the number of carbon atoms incorporated is always larger than the number of incident atoms calculated from graphite evaporation. Since by definition the sticking coefficient cannot be higher than 1, this means that the above stated assumption of a sticking coefficient equal to 1 for the determination of the C incident flux was incorrect. Of course, this result poses the question of what is the actual sticking coefficient of carbon on Si substrates, which is beyond the scope of this paper. A possible explanation for the higher sticking of C atoms in B_xC_{1-x} with respect to pure C films for $x<0.5$ can be related to the higher reactivity of the B-C bonds with respect to C-C.

Also, it has been determined by *ab initio* calculations that the B-C bond lengths are slightly larger than the C-C bond
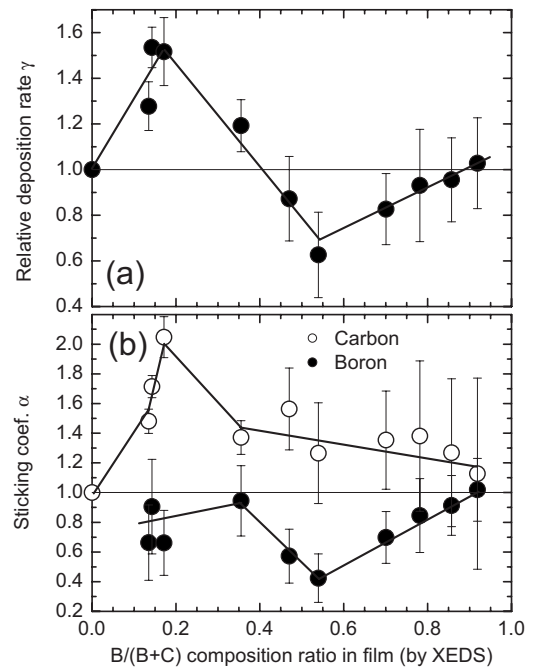
FIG. 3. Dependence with the film composition of (a) normalized growth rate relative to the evaporation rate γ and (b) sticking coefficients α of B and C atoms.
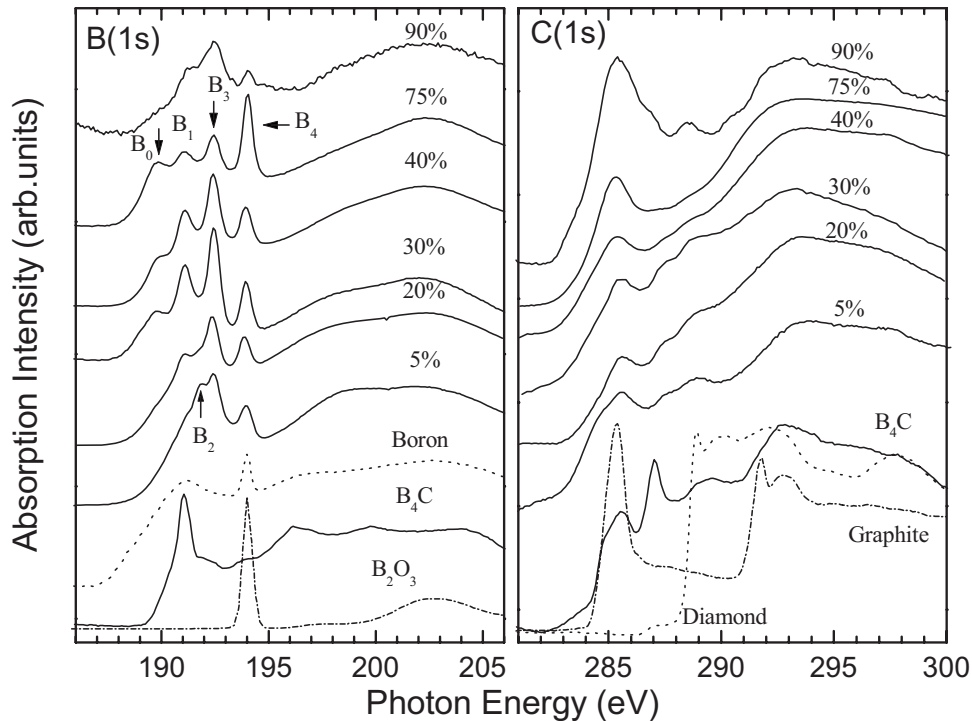
FIG. 4. B(1*s*) and C(1*s*) core level photoabsorption spectra of B_xC_{1-x} compounds. The curves are labeled with the names of the reference compounds and the carbon at. % in each B_xC_{1-x} sample. Up to five different bonding environments are distinguished in the B(1*s*) edge.

lengths in hexagonal BC_3.[14] As we shall see in the next section, a hexagonal structure is present in the coatings when $\gamma > 1$, corresponding to composition values between BC_6 and BC_2 Therefore, we might expect a different bonding distance in the hexagonal BC systems with respect to that of pure C. This could induce a compressive stress in the hexagonal network and compensate the local atomic stress of C atoms with sp^2 hybridization, which is preferentially tensile.[23] This fact would reduce the internal stress of the resultant BC films. Actually, coevaporated boron carbide coatings up to 2 μm thick have been grown with a $B/(B+C) < 0.4$ composition, while pure C films used to calculate Φ_C exhibited a thickness limit of 150 nm before delamination. Precedent works have shown that B doping relaxes the intrinsic strain in tetrahedral C based on similar arguments.[24]

The maximum γ value of ~1.6 is reached for $B/(B+C) \approx 0.17$, i.e., a BC_5 composition, and is also reflected in the α_C curve. For higher B contents, γ diminishes up to the minimum value of 0.65, which corresponds to a BC composition $B/C \sim 1$. This coincides with the decrease in the sticking coefficient of boron and carbon. Specifically, α_B reaches its minimum value or the maximum loss of B atoms. Therefore, the 1:1 stoichiometry is the less favorable from a chemical point of view.

To summarize, the behavior of the γ function for the B_xC_{1-x} compounds studied in this work can be separated into two regions. For film composition ratios $B/(B+C) < 0.4$, γ takes values greater than unity and is dominated by the variation in α_C, which also takes values greater than 1. For $B/(B+C) > 0.4$, γ is smaller than 1 due to loss of boron atoms as revealed by α_B. As we shall see in the following section, these two regions are connected to the structure of the B_xC_{1-x} compounds. The XANES study gives evidence of a graphiticlike bonding structure when the atomic concentration of carbon in the films is $C > 50\%$ and B_4C-like for $C < 50\%$.

B. Bonding structure of B_xC_{1-x} compounds

The XANES spectra of six different B_xC_{1-x} compounds are depicted in Fig. 4. The B(1*s*) and C(1*s*) core level absorption edges are indicated together with the reference spectra of boron, B_4C, B_2O_3, graphite, and diamond. The carbon content in atomic percentage of each sample is shown on top of the spectrum.

The B_4C reference spectra of Fig. 4 show no clear separation between the π^* and σ^* regions, either in the B(1*s*) or in the C(1*s*) absorption edge. This feature reflects a complex state of hybridization. The B(1*s*) edge starts at 189.0 eV and presents a narrow fingerprint peak at 190.9 eV on top of a background assigned to π^* states. The origin of this excitonic transition is still unclear. Jiménez *et al.*[4] suggested that this peak (labeled in their work as *A*) arises from boron in the icosahedra bonded to a CBC carbon atom or from boron in the chain itself. Furthermore, three additional peaks were reported in that work at 191.7 eV, labeled as B and assigned to B-rich carbide, at 192.3 eV, labeled as *C* and assigned to boron suboxide, and at 193.7 eV, labeled as *D* and assigned to boron oxide.

Regarding the C(1*s*) absorption edge of B_4C starting at 282.5 eV, a double peak at 284.9 and 285.6 eV is observed. Again from Ref. 4, these peaks are assigned to C atoms in the CBC chain. In principle, the proximity in energy of these features to the characteristic π^* transition of graphite could hinder us from distinguishing between BC_x and *a*-C forms. However, the whole shape of the spectrum is usually enough to solve this obstacle. For instance, the presence of the peak at 287.0 eV and the two shoulders at 288.5 and 291.0 eV due to C atoms in the icosahedra can be usually very helpful.

If we focus now on the coevaporated boron carbide compounds of this work, up to five different peaks can be distinguished in the B(1*s* → π^*) region of the XANES spectra

linked to resonant excitonic states. These peaks have been labeled as B_0-B_4 and appear at photon energies of 189.7, 191.0, 191.8, 192.4, and 194.0 eV, respectively. By direct comparison with the reference spectra, we observe that B_1 and B_4 coincide in energy with B_4C and B_2O_3 characteristic π^* states. Moreover, the energy of B_1-B_4 is similar to the A-D bonding environments described in Ref. 4. While peaks B_1, B_3, and B_4 appear in all the samples with different relative intensities, B_2 is only detected for the sample with a 5 at. % of C, supporting the assignment done in Ref. 4 for boron-rich boron carbides. Only peak B_0 does not correspond to any known BC-based reference material.

Precedent studies on hexagonal boron nitride have shown also four intense and sharp excitonic transitions in the π^* $B(1s)$ region but at slightly different energies.[25,26] These peaks were assigned to B atoms surrounded by 0, 1, 2, or 3 N vacancies in the sense of increasing energy, and probably occupied by other chemical species. We have extended this analysis of the $B(1s)$ transitions to our current study of BC compounds. Therefore, peaks B_0, B_1, B_3, and B_4 have been attributed to B-C_3, B-$C_2\otimes$, B-$C\otimes_2$, and B-$\otimes_3$ bonding environments in an sp^2 boron carbide structure, respectively. The symbol $\otimes$ is used to denote the C vacancy around the tricoordinated boron atom. The results discussed in the above paragraph support the idea that such vacancies are decorated with superficial oxygen contamination. Besides, the reported electron energy-loss spectrum of a BC_3 film shows a very intense peak at 190.1 eV in the B K edge, which is in agreement with the assignment of peak B_0.[15] Additionally, the relative intensity of B_0 is exactly maximum for the sample with a BC_3 composition.

Regarding the $C(1s)$ spectra, up to 30 at. % of C, the spectra look like the $C(1s)$ reference from boron carbide. Mainly three shoulders are detected at 285.6, 287.2, and 288.7 eV for this range of compositions. The first of them appears at the same energy as the peak assigned to C atoms in the CBC chain of boron carbide. The second corresponds to the narrow and intense peak observed in crystalline B_4C, which becomes broader and slightly shifted in energy in nonstoichiometric amorphous BC_x. The third is associated to the first σ^* shoulder mentioned for B_4C, which is also present in nonstoichiometric derivates.

When the C content increases, these features disappear and the graphite peak at 285.4 eV becomes dominant. This behavior suggests the graphitization of the samples. In fact, the $B(1s)$ edge reveals a similar change with composition. The shape of $B(1s)$ spectra is typical of an icosahedon-based structure for low C contents and develops to well resolved $1s \rightarrow \pi^*$ transitions with increasing C. This is followed by the appearance of a new B_0 bonding environment and the marked separation of the π^* and σ^* regions characteristic of hexagonal phases. The sample with 40 at. % of C is an in-termediate situation between a B_4C-like and a graphitic compound, which is close to the less stable composition B:C =1:1 discussed in the preceding section.

The XANES results show that the icosahedral B_4C-like structure remains as long as C represents less than ~50% of the total atomic composition. For stoichiometries richer in C than B, the structure tends to graphitize. These results are in agreement with the explanation given for the resistivity experiments reported in Ref. 18. Moreover, the $B(1s)$ and $C(1s)$ XANES spectra clearly prove that C is incorporated in the B_xC_{1-x} structure and not merely forming isolated graphitelike domains. In fact, no elemental phase segregation has been detected for any of the samples studied.

IV. CONCLUSIONS

Boron carbide compounds with any possible B_xC_{1-x} stoichiometry have been grown in this work by electron beam coevaporation with the substrate held at room temperature. This experimental setup gives us an accurate control over the composition of the films through the selection of the incident atomic flux of each element. A simple method for the determination of the impinging fluxes and the sticking coefficient of B and C has been presented. The sticking coefficient of evaporated C is lower than unity and increases when reacting with B atoms.

The reactivity of evaporated B and C atoms determined the deposition rate and the final composition and structure of the boron carbide films. In this way, two structural groups were identified by XANES as a function of the composition. When the x value is lower than 0.5 (i.e., C content higher than 50 at. %), the XANES spectra of the films demonstrates that the material is predominantly graphitic, while a B_4C-like structure is found for higher x. The transitional BC stoichiometry appears to be the less stable, with an intermediate structure between graphite and boron carbide.

Finally, new bonding environments in the XANES $B(1s)$ absorption edge typical of a BC_3 compound have been detected and tentatively assigned to B atoms in a hexagonal network with different numbers of C defects occupied by superficial O from contamination.

ACKNOWLEDGMENTS

*Corresponding author: Present address: Department of Physics, University of Antwerp, Campus One Eiken, Universiteitsplein 1, 2610 Wilrijk, Belgium. ignacio.caretti@ua.ac.be

[1] B. Morosin, T. L. Aselage, and R. S. Feigelson, *Novel Refractory Semiconductors*, MRS Sympocia Proceedings No. 97 (Materials Research Society, Pittsburgh, 1987), p. 145

[2] B. Morosin, G. H. Kwei, A. C. Lawson, T. L. Aselage, and D. Emin, J. Alloys Compd. **226**, 121 (1995).

[3] G. H. Kwei and B. Morosin, J. Phys. Chem. **100**, 8031 (1996).

[4] I. Jiménez, D. G. J. Sutherland, A. van Buuren, J. A. Carlisle, L. J. Terminello, and F. J. Himpsel, Phys. Rev. B **57**, 13167 (1998).

[5] R. Lazzari, N. Vast, J. M. Besson, S. Baroni, and A. Dal Corso, Phys. Rev. Lett. **83**, 3230 (1999).

[6] H. Werheit, R. Schmechel, S. O. Shalamberidze, G. I. Kalandadze, and A. Eristavi, J. Solid State Chem. **154**, 79 (1999).

[7] F. Mauri, N. Vast, and C. J. Pickard, Phys. Rev. Lett. **87**, 085506 (2001).

[8] M. Bouchacourt and F. Thevenot, J. Less-Common Met. **82**, 219 (1981).

[9] D. M. Bylander, L. Kleinman, and S. Lee, Phys. Rev. B **42**, 1394 (1990).

[10] D. Emin, Phys. Rev. B **38**, 6041 (1988).

[11] G. Fsanchini, J. W. McCauley, and M. Chhowalla, Phys. Rev. Lett. **97**, 035502 (2006).

[12] Q. Hu, Q. Wu, Y. Ma, L. Zhang, Z. Liu, J. He, H. Sun, H. Wang, and Y. Tian, Phys. Rev. B **73**, 214116 (2006).

[13] J. Kouvetakis, R. B. Kaner, M. L. Sattler, and N. Bartlett, J. Chem. Soc., Chem. Commun. **1986**, 1758.

[14] D. Tomanek, R. M. Wentzcovitch, S. G. Louie, and M. L. Cohen, Phys. Rev. B **37**, 3134 (1988).

[15] K. M. Krishnan, Appl. Phys. Lett. **58**, 1857 (1991).

[16] H. Yanagisawa, T. Tanaka, Y. Ishida, M. Matsue, E. Rokuta, S. Otani, and C. Oshima, Phys. Rev. Lett. **93**, 177003 (2004).

[17] Z. Liu, J. He, J. Yang, X. Guo, H. Sun, H. Wang, E. Wu, and Y. Tian, Phys. Rev. B **73**, 172101 (2006).

[18] K. Shirai, S. Emura, S. Gonda, and Y. Kumashiro, J. Appl. Phys. **78**, 3392 (1995).

[19] S. Schiller, U. Heisig, and S. Panzer, *Electron Beam Technology* (Wiley, New York, 1982).

[20] G. L. Köllogg, Surf. Sci. Rep. **21**, 1 (1994).

[21] I. Jiménez, I. Caretti, Z. Martín, and N. Fanegas. (unpublished).

[22] R. C. Weast, *Handbook of Chemistry and Physics* (CRC, Boca Raton, 1973).

[23] P. C. Kelires, Phys. Rev. Lett. **73**, 2460 (1994).

[24] M. Chhowalla, Y. Yin, G. A. J. Amaratunga, D. R. McKenzie, and Th. Frauenheim, Appl. Phys. Lett. **69**, 2344 (1996).

[25] I. Jiménez, A. Jankowski, L. J. Terminello, J. A. Carlisle, D. G. J. Sutherland, G. L. Doll, W. M. Tong, J. D. K. Shuh, and F. J. Himpsel, Appl. Phys. Lett. **68**, 2816 (1996).

[26] I. Jiménez, A. F. Jankowski, L. J. Terminello, D. G. J. Sutherland, J. A. Carlisle, G. L. Doll, W. M. Tong, D. K. Shuh, and F. J. Himpsel, Phys. Rev. B **55**, 12025 (1997).